Spinons and holons: a class of simple models

1992 J. Phys.: Condens. Matter 4 6819

(http://iopscience.iop.org/0953-8984/4/32/017)

J. Phys.: Condens. Matter 4 (1992) 6819–6844. Printed in the UK

Spinons and holons: a class of simple models

S C Y Siak† and M W Long‡

† Rutherford Appleton Laboratory, Chilton, Didcot, Oxon OX11 0QX, UK
‡ School of Physics, University of Bath, Claverton Down, Bath BA2 7AY, UK

Received 13 September 1991, in final form 23 December 1991

Abstract. In this paper, we discuss a class of quasi-one-dimensional models containing both spins and charge, which share the same generic solutions. In particular, we concentrate on a Heisenberg model of a topologically frustrated antiferromagnet, and a d–p model for oxygen hole hopping in a subgeometry of the copper–oxygen plane of the perovskite superconductors. The outstanding feature of these models lies in the simplicity of their solutions: their ground states are exact and contain uncorrelated, short-ranged singlet pairs. Excitations in these models fall into two distinct classes, namely, spin-$\frac{1}{2}$ chargeless domain-wall excitations or 'spinons', together with their conjugate excitations, which take the form of spin-$\frac{1}{2}$ chargeless 'antispinon' domain walls in the Heisenberg model, and spinless charge $+e$ hole excitations or 'holons' in the d–p model. In the case of the Heisenberg model, we have successfully constructed a sufficiently simple representation for the 'spinon' excitation which allows us to calculate its dispersion using elementary methods. This is therefore a concrete example of a 'spinon' excitation for which explicit representation has been possible.

1. Introduction and motivation

It is now widely accepted that the basic properties of ordinary unfrustrated (i.e. bipartite) Heisenberg antiferromagnets may be understood in simple, essentially classical terms [1]. Even in the extreme quantum mechanical limit of such a magnet being made up of spin-$\frac{1}{2}$ atoms, quantum mechanical fluctuations appear to have a minor effect, and the corresponding ordered ground state is Néel-like, with spins being in antiparallel arrangement along an arbitrary axis of quantization. The character of this ground state provides us, moreover, with information about the nature of its excitations: the Néel state has a (quasi)-infinite degeneracy associated with allowed rotations of the axis of spin quantization, and it is known from Goldstone's theorem [2], which applies in such systems, that the excitations must correspondingly be gapless. The lowest-lying excitations in fact represent small precessions of the axis of spin quantization which propagate through the system in the form of very low-frequency waves; the so-called spin waves.

Frustrated Heisenberg antiferromagnets, on the other hand, do not present such a well understood case. For instance, there is as yet no conclusive evidence, either theoretical or experimental, as to the nature of the ground state of a topologically frustrated two-dimensional antiferromagnet with spin-$\frac{1}{2}$ atoms, although it is believed that such a ground state probably does not exhibit the continuously broken symmetry expected classically and that it is in a real sense intrinsically quantum mechanical. As

0953-8984/92/326819+26$04.50

an example, experiments on the layered compound $SrCr_{8-x}Ga_{4+x}O_{19}$, which contains planes of magnetic spin-$\frac{3}{2}$ chromium ions that are connected in the form of a frustrated Kagomé net, suggest the absence of Néel ordering in the ground state [3]. Instead, the short-ranged magnetic correlations that are found, with correlation lengths of the order of 7 Å indicate a ground state with discretely broken symmetry. It is possible that the antiferromagnetic ground state for a collection of spin-$\frac{1}{2}$ atoms on a triangular lattice may likewise not exhibit continuous rotational degeneracy; in the case of the latter, a resonating-valence-bond (RVB) ground state has in fact been conjectured [4], although a signature of such an RVB state has not been detected experimentally. Both the quantum mechanical ground states postulated above are radically different from their classical analogues: the continuously broken symmetry which characterizes the latter is replaced in the former by a discrete symmetry breaking. Goldstone's theorem is not essential in such systems, and this in turn allows (but does not necessitate) the possibility of gapped excitations.

A major factor which has hitherto hampered progress in our understanding of frustrated antiferromagnets has been the paucity of simple, tractable models with exact solutions. In this paper, we present a quasi-one-dimensional, topologically frustrated Heisenberg antiferromagnet which has as its most distinctive feature unusually simple, purely quantum mechanical solutions. In particular, the lowest-energy solution is exact: there are two degenerate ground states, each consisting of uncorrelated short-ranged singlet or dimer pairs. The simplicity of this ground state allows us to elucidate the elementary excitations of the model rather thoroughly. We find a gap to excitations, which we interpret as being due to the formation of spin-$\frac{1}{2}$ domain walls. We also find that, due to a topological asymmetry in our model, there are *two classes* of domain wall present: one class incurs an energy cost and exhibits dispersion, whilst the second class costs no energy to create and is dispersionless. The first class of domain wall provides us with examples of the type of excitation known in the literature as spinons [5], and the second class of domain wall, being conjugate to the first, will therefore be henceforth referred to as antispinon.

Our motivation for introducing this particular magnetic model stems first from the simplicity of its ground state, which allows us to construct almost exact representations for its spinon excitations, and secondly from the fact that there appears to be an entire class of one-dimensional models, including some containing mobile charged vacancies or holes, which exhibit the same generic solutions as those described above. In particular, we discuss two quasi-one-dimensional models of direct relevance to high-temperature superconductivity, whose lowest-energy solutions are exactly analogous to those of our Heisenberg model. In these high-T_c models, short-ranged singlet correlations between spins are induced via the motion of charged vacancies. The resulting ground states exhibit the broken symmetry reminiscent of our Heisenberg model, and their elementary excitations also fall into two distinct, asymmetric classes. In the case of the high-T_c models, these excitations consist of spin-$\frac{1}{2}$, chargeless domain walls (spinons) together with spinless, charge $+e$ vacancy excitations (holons/antispinons).

We note, however, that none of the models in this class can undergo a superconducting transition. Their strength, namely the simplicity of their solutions, is mainly a consequence of constraints imposed by their topology and their one-dimensionality, but unfortunately these same topological constraints prevent any two charged excitations in the models from approaching one another, which in turn means that charge-pairing fluctuations *cannot* occur.

Nonetheless, there are two key features in our models which we believe on experimental grounds to be generic to the superconducting cuprates, namely a charge-carrier-induced paramagnetic ground state, and an energy gap to *magnetic* excitations. Our justification for the above claim, which we will now discuss, is based on the results of neutron scattering as well as NMR measurements. We stress at the outset that some of the experimental results which we discuss shortly are not clear-cut; indeed, many of the issues remain controversial, but we feel nevertheless that these rather intriguing results should not simply be dismissed, and offer in this paper a theoretical model which appears to be consistent with them.

Firstly, it is now known [6] that the undoped cuprates are antiferromagnetic insulators with spins which reside on the Cu sites, and that when these materials are doped with holes, which appear to be at the O sites, the antiferromagnetic correlations are destroyed. However, the concentration of doped holes need not be high before anitferromagnetic order disappears; for instance [7], in $La_{2-x}Sr_xCuO_4$, magnetism is essentially destroyed when 2.5% of the La atoms have been replaced by Sr, which corresponds to holes sitting at about 1 in 40 of the O sites. Moreover, inelastic neutron scattering experiments indicate that the Cu spins are preserved at this level of doping, but since the correlations between them largely appear to have been destroyed, it is natural to assume a paramagnetic state for the Cu moments.

Secondly, and more controversially, there is evidence from both inelastic neutron scattering [8] as well as NMR [9] experiments that a gap opens up in the spin excitation spectrum at temperatures well *above* T_c. One example of an experiment which can probe these magnetic excitations was performed by Shirane *et al* [8] on $La_{2-x}Sr_xCuO_4$ using neutrons. They measured the output intensity of the (magnetically) scattered component, integrated this output over *all* relevant angles, and studied the integrated intensity as a function of temperature. This integrated intensity, which is essentially a measure of the number of magnetic excitations present, was found to exhibit a dramatic decline at about 150 K in $La_{2-x}Sr_xCuO_4$, for which T_c by contrast is approximately 33 K. These results, if correct, suggest a gap opening up in the magnetic excitation spectrum, in contradistinction to the superconducting gap. We stress again that controversy still surrounds the above results, but more recent work by Rossat-Mignod's group [8] in fact appears to confirm the presence of a spin excitation gap.

Excitation gaps have previously been found by theoreticians to occur in quantum mechanical spin systems [10], most notably in spin-$\frac{1}{2}$ systems in which frustration is caused not by lattice topology but by the presence of conflicting interactions between the spins. There is in fact an exactly solved model—the so-called Majumdar–Ghosh chain [10], in which spin-$\frac{1}{2}$ atoms are coupled not just via nearest-neighbour interactions but also via next-nearest-neighbour interactions, with the bond strength of the latter being exactly half that of the former. Solutions of the Majumdar–Ghosh chain are very similar to those of our models [10]. Like our models, the Majumdar–Ghosh chain has a twofold degenerate, broken-symmetry ground state containing uncorrelated, short-ranged singlet pairs. There is similarly a gap to its excitations which can be interpreted as being due to the formation of spin-$\frac{1}{2}$ domain walls. However, the lack of topological asymmetry in the chain means that only one class of domain wall is created. Hence excited states of the Majumdar–Ghosh chain contain many equivalent spin-$\frac{1}{2}$ domain walls, and it turns out that such states are in fact much more difficult to analyse than the corresponding states in our models which contain distinct classes of excitations.

The rest of our discussion is divided as follows. In section 2, we introduce the topologically frustrated Heisenberg antiferromagnetic model which forms the crux of this paper. We concentrate in particular on trying to understand the gapped excitations in our mode. We present detailed analytical and numerical evidence for the two classes of spin-$\frac{1}{2}$ domain wall in the model. We then show that the solutions for our Heisenberg antiferromagnet are not uniquely restricted to a specific model but are in fact generic to a whole class of one-dimensional systems. In section 3, we discuss two electronic systems containing mobile charged vacancies: a t–J model for hole hopping on a frustrated, quasi-one-dimensional lattice, and a d–p model for hole motion on a restricted sub-geometry of the Cu–O plane of the perovskite superconductors. We show in both the above cases that the ground states contain uncorrelated, short-ranged singlet pairs and that the excitations fall into two distinct classes. In section 4, we conclude with a brief summary.

2. An exactly solvable spin-$\frac{1}{2}$ Heisenberg model: spinon and antispinon excitations

In this section, we discuss a quasi-one-dimensional, quantum mechanical Heisenberg model of an antiferromagnet which has unusually simple solutions. The model contains spin-$\frac{1}{2}$ atoms, each of which is assumed to interact only with its nearest neighbours via the Heisenberg exchange. The atoms in our model are situated at the sites of a lattice with topological frustration, namely the linear chain of triangles shown in figure 1. We will henceforth refer to this configuration as the sawtooth topology, and will regard the sawtooth as being made up of a chain of backbone atoms connected to vertex atoms (cf figure 1).

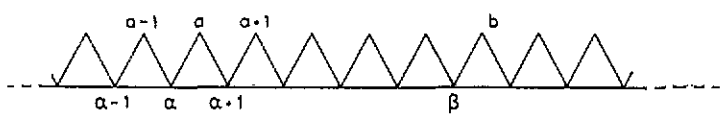

Figure 1. The one-dimensional lattice of triangles which we refer to as the sawtooth. 'Vertex' sites are denoted by Roman lettering, while 'backbone' sites are denoted by Greek lettering.

Our starting point is the Heisenberg Hamiltonian

$$H = J \sum_{\langle i,j \rangle} \boldsymbol{S}_i \cdot \boldsymbol{S}_j \tag{2.1a}$$

which for the sawtooth topology can be expressed in terms of the total spin of the atoms in each independent triangle:

$$H = \frac{J}{2} \sum_{T} \boldsymbol{S}_T \cdot \boldsymbol{S}_T - \frac{9}{8} J N_T. \tag{2.1b}$$

In the above equations, $\boldsymbol{S}_i = \frac{1}{2} c^\dagger_{i\sigma} \boldsymbol{\sigma}_{\sigma\sigma'} c_{i\sigma'}$ denotes the spin operator at the ith lattice site, $c^\dagger_{i\sigma}$ being the operator which creates an electron of spin σ at the ith lattice site ($c_{i\sigma}$ is its conjugate operator) and $\boldsymbol{\sigma}$ being the Pauli operator. In addition, J is the coupling parameter between any nearest-neighbour pairs of spins, denoted

by the brackets $\langle\rangle$, S_T represents the total spin in a triangle, N_T is the total number of triangles, and the summation is either over all pairs of nearest-neighbour spins, as in (2.1*a*), or alternatively, over all triangles in the lattice, as in (2.1*b*).

Our main motivation for examining the above model lies in the fact that it exhibits solutions which are especially simple. In particular, its ground state is exact, and there is therefore the possibility of obtaining a simple picture for its excitations.

We probe the above spin system via a mixture of analytical as well as numerical techniques, which we will describe in greater detail in the course of our discussion.

The ground state of the sawtooth model has been described elsewhere [11], but we include an account here for completeness. The ground state is double degenerate and consists of uncorrelated, short-ranged singlet pairs (see figures 2(*a*) and (*b*)). It is important to note that there is absolutely no correlation between any two pairs of singlets, not even between nearest-neighbour pairs. In other words, $\langle S_i \cdot S_j \rangle = 0$ for any i, j lying on different triangles, and this ground state can be written down exactly.

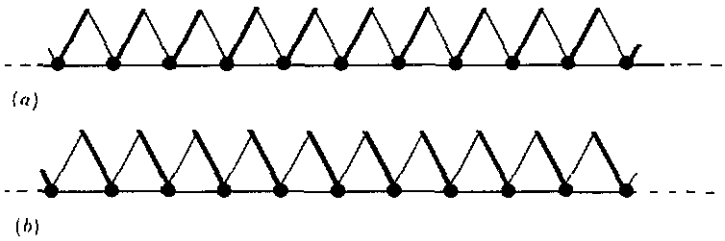

Figure 2. The exact, doubly degenerate ground states of our Heisenberg model. All spins on the lattice are paired up into short-ranged singlets or valence bonds (denoted in bold), and the ground state exhibits the broken symmetry shown.

We can understand the above result for the ground state by observing that the Hamiltonian for the sawtooth (2.1*b*) is minimized by independently minimizing the total spin in each triangle. Quantum mechanically, this means that the total spin in every triangle is $\frac{1}{2}$, leading to a ground state energy of

$$E_g = -\tfrac{3}{4} J N_T \tag{2.2}$$

which depends only on the number of triangles in the system. A total spin of $\frac{1}{2}$ in each triangle can, in turn, be achieved by having, in every triangle, one nearest-neighbour singlet pair and one unpaired spin which is then free to bind into a singlet pair with a spin in the next (adjacent) triangle, and so on, thus forming the ground state of independent singlets of figure 2. In principle, other possibilities, such as states containing longer-ranged singlet pairs, cannot be excluded, but the only low-spin states which exhibit a local broken symmetry are the ones depicted in figure 2, and we can prove numerically that they do indeed form the preferred ground state.

It is interesting to note that this quantum mechanical ground state is radically different from its classical counterpart, which is instead made up of [11] a superposition of infinitely many possible states containing spins pointing in directions that are at 120° with respect to each other. (Such states are said to contain long-ranged, non-collinear magnetic ordering.)

We now turn to our main concern in this section, namely the spin excitations in our Heisenberg model. Let us begin our discussion by stating three numerical results, obtained from calculations on small clusters with translational invariance. Firstly, we

find an energy gap between the ground state and the lowest band of excited states, with the magnitude of this gap being approximately 0.2 J (figure 3(*a*)). Secondly, we find that the lowest band of excited states (which contains as many states in it as there are unit cells in the lattice) exhibits a flat energy spectrum, i.e. the $E(K)$ versus k dispersion curve scales to become flat (figure 3(*b*)), in which we plot the width of the first band as a function of inverse system size. Thirdly, our numerical calculations show that the lowest band of excited states belongs to the subspace of spin states with total spin 1.

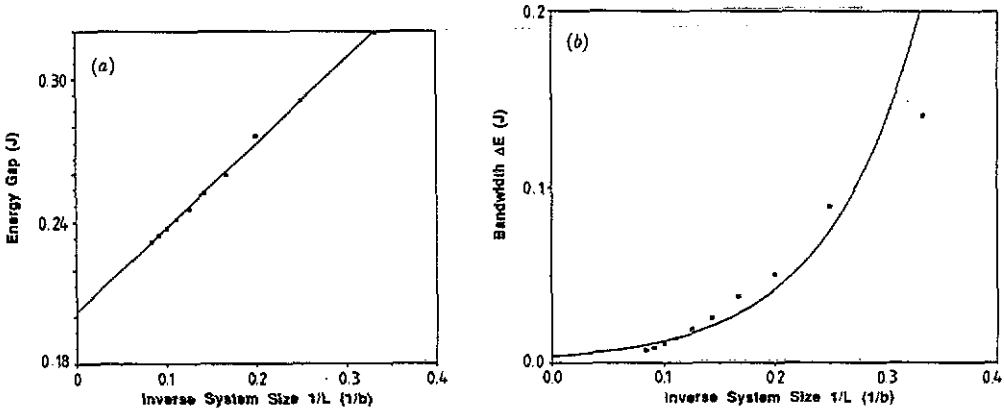

Figure 3. (*a*) The energy gap between the ground state and the first band of excited states, plotted as a function of inverse system size, for systems containing up to 24 spins. The linear extrapolation shown leads to an energy gap of 0.20 J for an infinite system. $y = 0.20180 + 0.35579x$, $R^2 = 0.998$. (*b*) The width of the first band of excited states, plotted as a function of inverse system size. This first band is clearly flat. $y = 3.7708e^{-3} \times 10^{5.2003x}$, $R^2 = 0.938$.

Given the nature of the ground state, it is natural to interpret the presence of a gap to excitations as being due to the formation of domain walls in the system: in order for the domain walls to form, it is necessary for the singlet pairs in the ground state to break up, thereby incurring a finite, non-zero energy cost. In a system with periodic boundary conditions such as ours, domain walls must in fact be created in pairs, the second domain wall being required to restore translational invariance. Since the lowest band of excited states has total spin 1, it follows that if these states do indeed contain two domain walls, then each of the domain walls must have spin $\frac{1}{2}$. Our picture for an eigenstate lying in the first band is that it contains two spin-$\frac{1}{2}$ domain walls as anticipated, but unlike other models in which a spin-1 excitation is known to split up into two identical spin-$\frac{1}{2}$ excitations, ours contains a topologial asymmetry: it would appear that our domain walls fall into two distinct classes. The first class of domain wall in our model costs no energy to create and exists as a localized excitation, whilst the second class of domain wall, which costs approximately 0.2 J to create, has a finite, non-zero coherence length and is delocalized around the (localized) domain wall. We will henceforth refer to the second class of excitation as the spinon, whilst the first class of excitation, being conjugate to the spinon, we will call the antispinon excitation.

In the rest of this section, we will justify the above interpretation by presenting both analytical as well as numerical evidence in its support. We will divide our

discussion into two further subsections for easier reading. Our analytical calculations form the crux of this work and are presented first, in subsection 2.1, to be followed by numerical results in subsection 2.2.

2.1. Analytical calculations

We begin this subsection by discussing the antispinon excitation, which we will show incurs no energy cost and exhibits a flat energy spectrum.

Let us consider the many-spin state $|\Phi_\alpha\rangle$ depicted in figure 4, in which all the spins are paired into local, short-ranged singlets except for the spin at the αth backbone site. There are three points to note about $|\Phi_\alpha\rangle$. Firstly, $|\Phi_\alpha\rangle$ differs from the ground state shown in figure 2 precisely because of the presence of the unpaired spin: the ground state with all its singlet pairs belongs to the spin 0 subspace, whilst $|\Phi_\alpha\rangle$ with its single unpaired spin belongs to the subspace of spin $\frac{1}{2}$. Secondly, $|\Phi_\alpha\rangle$ contains a domain wall in the form of the unpaired spin—the unpaired spin separates two regions with singlet pairs pointing in 'opposite' directions (figure 4) and in this respect, acts as a domain wall. We will return to this point in subsection 2.2. Thirdly, $|\Phi_\alpha\rangle$ is clearly only one member of a large set, denoted $\mathcal{M}$, of many-spin states in which all spins bar one are paired up locally into short-ranged singlets, each member of the set differing from one another only in the position of the unpaired spin and not in the number of singlet pairs that they contain.

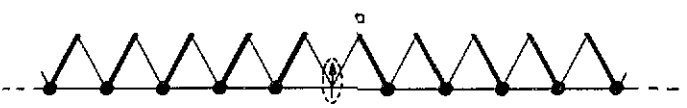

Figure 4. The state $|\Phi_\alpha\rangle$ in which all spins are paired up with their nearest neighbours into singlets, except for the spin at the αth backbone site. The state shown belongs to the set $\mathcal{M}$ (see text).

For the state $|\Phi_\alpha\rangle$, it is easy to prove that

$$H|\Phi_\alpha\rangle = E_g|\Phi_\alpha\rangle \tag{2.3}$$

i.e. that $|\Phi_\alpha\rangle$ is an exact eigenstate of the Heisenberg Hamiltonian on the sawtooth lattice, with the eigenvalue E_g being precisely equal to the ground state energy of (2.2).

Let us try to understand the above result. To see that $|\Phi_\alpha\rangle$ must indeed be an exact eigenstate of the above Hamiltonian, one need only consider a single triangle: for a Heisenberg antiferromagnet with only nearest-neighbour interactions, one singlet pair together with one free spin in a triangle constitutes an exact eigenstate, hence the state $|\Phi_\alpha\rangle$, which contains one singlet pair and one free spin in every triangle, must correspondingly be an exact eigenstate. To understand why $|\Phi_\alpha\rangle$ is energetically the same as the ground state, we note that $|\Phi_\alpha\rangle$ can be formed by adding one unpaired spin to the configuration of ground state singlet pairs, without breaking up any singlet pairs. Consequently, the presence of the domain wall in the state $|\Phi_\alpha\rangle$ does not incur an energy cost, and this is the class of domain wall which we refer to as the antispinon.

We also note that since the above arguments are independent of the position of the unpaired spin, it follows that they must hold not just for $|\Phi_\alpha\rangle$ but for any state

belonging to the set $\mathcal{M}$. There is therefore a whole set of equations analogous to (2.3); one for every member of the set $\mathcal{M}$, all of which have the same eigenvalue E_g. In other words, we expect the spin states considered above to exhibit a huge degeneracy, and this leads to interesting consequences.

Suppose we construct normalized Bloch functions

$$|\Phi_k\rangle = \left(\frac{1}{N_k}\right)\sum_\alpha \exp(\mathrm{i}\boldsymbol{k}\cdot\boldsymbol{R}_\alpha)|\Phi_\alpha\rangle \tag{2.4a}$$

out of the states in the set $\mathcal{M}$, in which the normalization factor N_k, is found by calculation to satisfy

$$N_k^2 = \sum_\alpha\sum_\gamma \frac{1}{2}^{|\boldsymbol{R}_\gamma-\boldsymbol{R}_\alpha|}\exp\left[\mathrm{i}\boldsymbol{k}\cdot(\boldsymbol{R}_\alpha-\boldsymbol{R}_\gamma)\right]. \tag{2.4b}$$

We could obviously construct one Bloch function for every allowed wavevector $\boldsymbol{k}$, and the Bloch functions thus obtained can be shown to be orthogonal to one another. The interesting point to note is that because of the degeneracy of the constituent spin states, we find

$$H|\Phi_k\rangle = \left(\frac{1}{N_k}\right)\sum_\alpha \exp(\mathrm{i}\boldsymbol{k}\cdot\boldsymbol{R}_\alpha)H|\Phi_\alpha\rangle = E_g|\Phi_k\rangle \tag{2.5}$$

for any $\boldsymbol{k}$; that is, each Bloch function associated with a different wavevector $\boldsymbol{k}$ is itself an exact eigenstate, and that moreover all these Bloch functions are degenerate in energy with eigenvalue E_g. Consequently, the antispinon that is described by a wavepacket of these Bloch functions has a flat energy band associated with it.

What implications do such a flat band have for the antispinon excitation in real space? One could answer this question by constructing an antispinon wavepacket in real space, and an obvious way of achieving this is by transforming the reciprocal-space Bloch functions above back to real space via

$$|\Phi_\beta\rangle_W = \frac{1}{N}\sum_{\boldsymbol{k}}\sum_\alpha \frac{1}{N_k}\exp\left[\mathrm{i}\boldsymbol{k}\cdot(\boldsymbol{R}_\alpha-\boldsymbol{R}_\beta)\right]|\Phi_\alpha\rangle. \tag{2.6}$$

This procedure gives us a Wannier orbital which is centred on, or 'localized', at the lattice site β, but which has a finite, non-zero spread over neighbouring lattice sites. The finite radius of such an orbital corresponds physically to a finite region of coherence for the antispinon domain wall that is represented by the Wannier wavepacket. One can readily show that these real-space Wannier orbitals, like their reciprocal-space Bloch counterparts, form an orthogonal set.

The important point is that, again

$$H|\Phi_\beta\rangle = E_g|\Phi_\beta\rangle \tag{2.7}$$

for any β. Hence the Wannier orbital thus constructed is also an exact eigenstate of our Hamiltonian with eigenvalue E_g. Consequently, if the antispinon is initially coherent within a certain region of the sawtooth lattice, (the length scale of this region being set by the radius of the corresponding Wannier orbital), then the antispinon

will remain localized in that region. On the other hand, since the Wannier orbitals centred at the different lattice sites β are all degenerate with eigenvalue E_g (i.e. a flat band), it costs no energy for the domain wall to be in another region of the lattice, and its centre of localization is arbitrary.

In the above discussion, we used as our basis a set of states containing many spins, in which the spins are paired up into local singlets. It will turn out to be natural for us to use, as the basis set in our second analytical calculation, a set $\mathcal{N}$ of spin states with short-ranged singlet pairs (a member of this set is depicted in figure 5(*a*)), which is not equivalent of $\mathcal{M}$ but is in some sense complementary to it. Both sets of states $\mathcal{M}$ and $\mathcal{N}$, in fact, share the same two problems, namely overcompleteness and non-orthogonality.

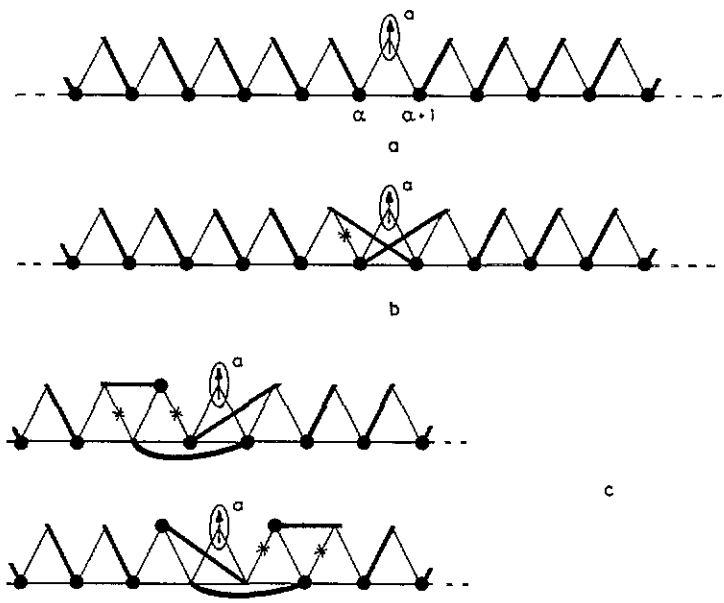

Figure 5. (*a*) The state $|\Psi_a\rangle$ in which all spins are paired up into short-ranged singlets except for the spin at the ath vertex site. This state belongs to the set $\mathcal{N}$ (see text). (*b*) The state $|\Psi'_a\rangle$ generated after one iteration. Note the appearance of long-ranged singlets. The asterisk denotes a symmetrized bond. (*c*) Two of the long-ranged singlet states included in $|\Psi'_k\rangle$. Once again, bonds with asterisks have been symmetrized.

We illustrate these problems by considering states in the set $\mathcal{M}$. The overcompleteness can be seen easily by noting that the amplitude of finding the unpaired spin on the ath vertex site is linearly dependent on the amplitudes of finding it on the nearest-neighbour αth and $(\alpha+1)$th backbone sites:

$$|\Phi_a\rangle = |\Phi_\alpha\rangle - |\Phi_{\alpha+1}\rangle. \tag{2.8}$$

One immediate consequence of this is that there are only as many degenerate states in $\mathcal{M}$ as there are backbone sites on the lattice, whereas one might naively have assumed this degeneracy to be equal to the total number of sites on the lattice.

The non-orthogonality of the states belonging to $\mathcal{M}$ becomes obvious when one calculates the overlap between its members, for instance

$$\langle\Phi_{\alpha+1}|\Phi_\alpha\rangle = \tfrac{1}{2} \qquad \langle\Phi_a \mid \Phi_\alpha\rangle = \tfrac{1}{2} \tag{2.9}$$

and so on. One could, if one desired, construct an orthogonal basis set from these short-ranged singlet states, for instance by forming Wannier orbitals as we did in (2.4). We shall, however, continue using states with local singlets instead of working with an orthogonal basis, because short-ranged singlet states like these turn out to provide a better description for both classes of excitation in our model than do the Wannier orbitals.

We have therefore shown that there is one type of spin-$\frac{1}{2}$ domain wall present in our model, which we have called the antispinon, and which costs no energy to create, essentially because its formation does not require breaking up any of the singlet pairs present in the ground state. Moreover, we have shown that the antispinon has a flat energy band associated with it and can therefore exist as a localized excitation. However, because of this flat band, its centre of localization is perfectly arbitrary on the lattice.

Let us now discuss the second domain wall that is present in our system, which we will show costs approximately 0.2 J to create and has a non-trivial energy spectrum associated with it. It is useful for us at this point to consider the many-spin state $|\Psi_a\rangle$ (figure 5(*a*)) belonging to the set $\mathcal{N}$, which contains a single domain wall on the ath vertex site with all other spins paired up in local singlets. Note that $|\Psi_a\rangle$ is rather different from the state $|\Phi_\alpha\rangle$ discussed previously in connection with the first domain wall: there is one less singlet in $|\Psi_a\rangle$, since the singlet pair present in the ath triangle in $|\Phi_\alpha\rangle$ is absent in $|\Psi_\alpha\rangle$. Applying our Heisenberg Hamiltonian to $|\Psi_a\rangle$, we can show that

$$H|\Psi_a\rangle = E_0 J|\Psi_a\rangle + (J/2)[\tfrac{5}{2}|\Psi_a\rangle - |\Psi_{a-1}\rangle - |\Psi_{a+1}\rangle + |\Psi'_a\rangle] \tag{2.10a}$$

and we see immediately that $|\Psi_a\rangle$, unlike $|\Phi_\alpha\rangle$, is not an eigenstate of our Hamiltonian. Instead, the application of the Heisenberg Hamiltonian to $|\Psi_a\rangle$ moves the domain wall on the ath vertex site to neighbouring sites, and in the process generates the states $|\Psi_{a-1}\rangle$ and $|\Psi_{a+1}\rangle$, together with the state $|\Psi'_a\rangle$ depicted in figure 5(*b*), which contains longer-range singlet pairs. We note here that $|\Psi'_a\rangle$ has been constructed in such a way that it is orthogonal to all three of $|\Psi_a\rangle$, $|\Psi_{a-1}\rangle$ and $|\Psi_{a+1}\rangle$.

It is as usual more convenient to work in reciprocal space, where (2.10*a*) becomes

$$H|\Psi_k\rangle = J[\tfrac{5}{4} - \cos(k\cdot R)]|\Psi_k\rangle + (J/2)|\Psi'_k\rangle \tag{2.10b}$$

in which $|\Psi_k\rangle$ and $|\Psi'_k\rangle$ are the Fourier transforms of $|\Psi_a\rangle$ and $|\Psi'_a\rangle$ respectively, and where we have changed the zero of energy by subtracting E_0. If we neglect contributions from $|\Psi'_k\rangle$ in the first instance, we find that the domain wall represented by a wavepacket of the above states has a dispersion relation given by

$$E(k) = [\tfrac{5}{4} - \cos(k\cdot R)]J. \tag{2.10c}$$

This dispersion relation (curve I in figure 6) tells us that in a minimum energy of 0.25 J is required to create this second domain wall in our system, in contrast to the antispinon excitation previously discussed. The fact that our analytical calculation predicts an energy cost for the creation of the second class of domain wall (the 'spinon') is not surprising, given that an energy gap is anticipated in our numerical calculations. What is surprising is the accuracy with which our variational procedure

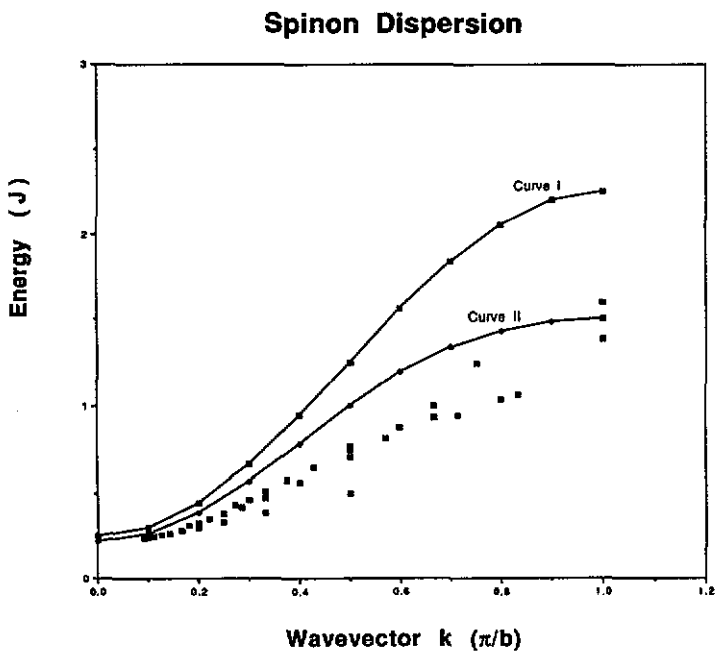

Figure 6. The results of our calculations of spinon energy as a function of wavevector are summarized on this graph. Curve I is obtained from an analytical calculation of spinon dispersion, accurate to one iteration. Curve II represents results of the same calculation carried out over two iterations. The results of this analytical calculation compare very well with numerical values for the spinon dispersion, which have been plotted as scatter points.

manages to predict this gap: even the lowest-order calculation above gives an energy gap of 0.25 J, which compares rather well with the numerical value of ~ 0.2 J.

When we include first-order corrections from the states $|\Psi'_k\rangle$ which contain even longer-ranged singlet pairs, our analytical calculation of the magnitude of this energy gap improves even more dramatically. We can show that

$$H|\Psi'_k\rangle = \tfrac{9}{4}J|\Psi'_k\rangle + \tfrac{1}{2}J[\tfrac{5}{4} - \cos(k\cdot R)]|\Psi_k\rangle + |\Psi''_k\rangle \qquad (2.10d)$$

where the states denoted by $|\Psi''_k\rangle$ are orthogonal to both $|\Psi'_k\rangle$ and $|\Psi_k\rangle$, and contain even longer-ranged singlet pairs which are generated as a result of a further delocalization of the domain wall from the αth vertex site to more distant sites. Examples of states that are included in $|\Psi''_k\rangle$ are shown in figure 5(*c*). If we now take contributions from the states $|\Psi'_k\rangle$ into account, but neglect terms derived from $|\Psi''_k\rangle$, we generate the Hamiltonian

$$H = J\begin{bmatrix} \tfrac{5}{4} - \cos(k\cdot R) & \tfrac{1}{2}(\tfrac{5}{4} - \cos(k\cdot R)) \\ \tfrac{1}{2} & \tfrac{9}{4} \end{bmatrix} \qquad (2.10e)$$

which, on diagonalization, results in the dispersion relation (curve II in figure 6)

$$E(k) = \tfrac{1}{2}[\tfrac{7}{2} - \cos(k\cdot R)] \pm \tfrac{1}{2}\sqrt{[\tfrac{7}{2} - \cos(k\cdot R)]^2 - 8[\tfrac{5}{4} - \cos(k\cdot R)]}. \qquad (2.10f)$$

There are two points to note about this dispersion curve. Firstly, the minimum energy required to create the spinon has been reduced to ~ 0.22 J, which gives

us the required energy gap to an extremely good approximation, even though we have only performed two iterations in our calculation. This must mean that our starting state, $|\Psi_a\rangle$, represents a good description of the spinon wavefunction, since all our assumptions appear consistent. Secondly, the spinon energy band has flattened considerably as a result of including the first-order contributions from states which contain long-ranged singlet pairs. Since long-ranged singlets are generated in our case by delocalizing the spinon away from its initial position in the lattice, we must conclude that the energy of the spinon can be reduced by allowing it to move over increasingly large regions in the system. This makes intuitive sense: roughly speaking, if we view the spinon moving within the background of spin singlets as behaving like a quantum particle in a box (albeit with some complicated potential to account for the spin background), then we can see just from simple arguments based on the uncertainty principle that a particle which is allowed to be delocalized over a larger region of space must correspondingly have a lower (kinetic) energy associated with it.

Hence we have shown that there are two classes of topological, spin-$\frac{1}{2}$ domain walls in our Heisenberg model: the antispinon excitations which incurs no energy cost, and the spinon excitation which costs at least 0.2 J to create. The antispinon has a flat energy band associated with it and is essentially a localized excitation. The spinon, in contrast, is characterized by a finite, non-zero coherence length, and its energy band is correspondingly non-trivial,

At this juncture, let us remind the reader that we were led to the above calculations by our numerical results, which show a band of states at approximately 0.2 J above the ground state, with total spin 1 and a flat spectrum. This last point is important, since a flat energy band is rather unusual and imposes constraints on any physical picture which one produces for the excitations. Our interpretation of these results is that states in the band contain two independent excitations; one spinon which is delocalized over a finite region of coherence, together with one antispinon which must be localized somewhere in the system in order for the energy spectrum of both excitations to be a flat band. In addition to the analytical results already presented, we will provide numerical evidence in the next section which supports our interpretation.

Before leaving this section, there is one last point which we must make concerning the excitations in our model, namely that the spinon introduced above is free to move around its conjugate, localized excitation (the antispinon), but the topology of the sawtooth lattice is such that the spinon is forbidden from ever moving past the antispinon. We can readily prove this to be the case by considering the state $|\Psi\rangle$ shown in figure 7, in which the spinon is situated to the right of the antispinon from the reader's viewpoint. If we calculate $H|\Psi\rangle$, we find that we never generate states in which the spinon has moved past the antispinon to its immediate left: the spinon can only arrive in that position by first moving away from the antispinon—to its right—and travelling once around the lattice. Hence we are led to a particularly simple picture for the excited states in our model in which spinon and antispinon domain walls 'concertina' against one other but do not exchange positions directly, and we emphasize again that such a simple picture is possible only because of the topology of the sawtooth lattice.

2.2. Numerical calculations

In this section we discuss the results of numerical calculations which support the above picture of spinon and antispinon excitations. Our numerical technique is straightfor-

Figure 7. A pictorial representation of a state in the first excited band, containing one spinon and one antispinon. On this diagram, the spinon has been placed to the right of the antispinon, facing the reader.

ward: we start by considering small clusters of atoms, generating the Heisenberg Hamiltonian within convenient sets of basis states and diagonalizing to obtain the eigenvalues and eigenstates. We then probe the nature of the solutions thus obtained by examining spin–spin correlations within them. We repeat our calculations for increasingly large clusters, and finite-size scale our results for physical quantities of interest, such as energies and spin–spin correlations.

Let us first present numerical evidence for the existence of two classes of domain wall. In order to illustrate our main points, we will discuss in detail some of the typical results obtained from calculations on small clusters of atoms.

Consider the small cluster of five triangles shown in figure 8(*a*). Solving numerically for this cluster with free boundary conditions, we find a whole range of eigenvalues and eigenstates, all of which have half-integer spin $S = \frac{1}{2}, \frac{3}{2}$, and so on. From within this set of eigensolutions, we observe that there are no fewer than six states, each having total spin $\frac{1}{2}$, which are all at the lowest energy of -3.75 J (cf (2.2) for the case of five triangles). On calculating correlations between nearest-neighbour spins in the cluster, we find that each of these degenerate states contains five uncorrelated singlet pairs (hence their energy of -0.75 J $\times$ 5 $=$ -3.75 J) together with one unpaired spin which acts as a domain wall (see, for instance, figure 8(*b*)). In addition, these spin–spin correlations tell us that the sixfold degeneracy of the lowest eigensolutions stems from the existence of six backbone sites on which the unpaired spin could be situated.

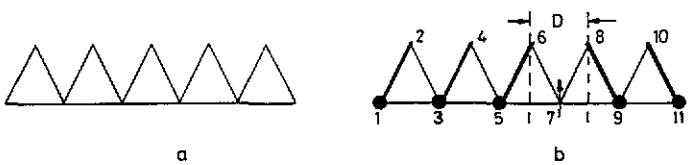

Figure 8. (*a*) A small cluster of five triangles: topology type I. (*b*) Exact eigenstate obtained numerically. The unpaired spin acts as a domain wall.

Such correlations and degeneracy are reminiscent of the antispinon excitation discussed in section 2.1, and our numerical results above clearly demonstrate the presence of one antispinon domain wall in the lowest eigensolution of the cluster of figure 8(*a*). However, results such as these are not specific to a cluster size of five triangles; similar characteristics are exhibited by the lowest eigensolutions of all calculable clusters with similar topology, provided free boundary conditions prevail. In our numerical work, clusters of up to 24 atoms are examined.

In addition, we have said that we find a whole range of eigenvalues and eigenstates for such clusters, some of which have total spin greater than $\frac{1}{2}$. Having interpreted the lowest degenerate eigensolutions as states containing one antispinon, it is natural for us to interpret the antispinon as being analogous to a single quantum mechanical particle in a box, and to view the higher cluster solutions as being the excited modes of the antispinon. There is, however, one subtlety which we will briefly mention here,

and which we will come back to. Although it has been convenient for us to use what is essentially a single-particle picture in interpreting the numerical results above, what we are really dealing with is a system containing many spins. Consequently, many-particle excitations are also allowed, and some of the higher excited states contain more than one domain wall.

Let us digress a little from our main discussion here to formalize somewhat our notion of a domain wall. A quantitative signature of a domain wall in our model appears in the correlations of nearest-neighbour spins, calculated along the vertex sides of the triangles that form the sawtooth. We should point out that these ideas apply equally well to both the spinon and the antispinon domain wall. Referring to figure 8(*b*), suppose we systematically calculate nearest-neighbour spin correlations on the 'left' vertex sides of the triangles, i.e. $\langle S_1 \cdot S_2 \rangle$, $\langle S_3 \cdot S_4 \rangle$, $\langle S_5 \cdot S_6 \rangle$, and so on. Plotting these correlations as a function of distance along the sawtooth, we obtain curve I in figure 9, where we have changed the zero of energy by adding a constant of 0.75 J. Curve I therefore gives us the probability of independently finding singlet pairs on the vertex sides 1–2, 3–4, and so on. Moreover, suppose now we repeat the above calculations, but this time for spin correlations on the 'right' vertex sides, i.e. $\langle S_2 \cdot S_3 \rangle$, $\langle S_4 \cdot S_5 \rangle$, $\langle S_6 \cdot S_7 \rangle$, etc. We find that a similar plot of correlations versus distance along the chain leads to a curve (II in figure 9) which is the mirror image of curve I above. The step-like quality of these curves and their symmetry indicates that the following dramatic changes, centred on the small region D in figures 8(*b*) and 9, occur in nearest-neighbour spin correlations: on the left of region D, singlet pairs are found on 'left' vertex sides of triangles, whilst spins on 'right' vertex sides are uncorrelated; on the right of D, singlet pairs lie on the 'right' vertex sides of triangles and spins on 'left' vertex sides are uncorrelated. The above changes are synonymous with the presence of a domain wall in region D, with the width of this region giving a measure of the coherence length of the domain wall. For the particular example being considered, the step functions are very abrupt, because the domain wall is assumed to be coherent only over one lattice spacing. It is reasonable to expect these ideas to also apply to a domain wall with a longer coherence length, as we will show below.

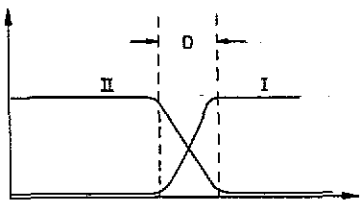

Figure 9. A plot of nearest-neighbour spin correlations as a function of distance along the cluster, as explained in the text.

We now discuss the small cluster of triangles with the topology shown in figure 10, which we will henceforth refer to generically as topology type II (in contradistinction to that of figure 8(*a*), which we will call topology I). Our motivation for choosing to examine topology II stems from the fact that the spinon and antispinon are conjugate excitations to each other in the same way that topology II is conjugate to that of topology I: if we connect up the two clusters of figures 8(*a*) and 10, we find that together they form a periodic sawtooth lattice containing twenty atoms.

Solving for the cluster of figure 10, we again obtain a whole range of eigenvalues and eigenstates, all of which have a half-integer spin of $\frac{1}{2}$, $\frac{3}{2}$, and so on. From this

Figure 10. A small cluster of five triangles: topology type II, which is complementary to that shown in figure 8(*a*).

set of solutions, we find that the lowest eigenstate is non-degenerate, has total spin $\frac{1}{2}$, and is at energy -3.4543 J. We note that this is 0.2957 J above that of its antispinon counterpart, which we showed earlier to have energy -3.75 J. When we examine the correlations between nearest-neighbour spins along the vertex sides of the cluster, we obtain a profile synonymous with that of a domain wall whose coherence length extends throughout the cluster.

These results suggest that the lowest eigensolution for the cluster of figure 10 contains one spinon domain wall, which in that particular cluster appears to cost 0.2957 J to create. The presence of this energy gap is important: the gap here is much larger than the value of ~ 0.2 J obtained in previous calculations, but this is not surprising given the small size of our cluster. When we repeat our calculations on increasingly large clusters of topology II and perform a finite-size scaling analysis of our results, we once again find an energy gap of approximately 0.2 J. We are therefore entirely consistent in regarding the lowest eigensolutions of generic clusters of topology II as containing one spin-$\frac{1}{2}$ spinon.

Given this interpretation, it is once again natural for us to think of the spinon in a small cluster as being like a particle in a box, and to view the higher eigensolutions of these clusters as representing either the excited modes of the spinon or states containing more than one spinon. Such a particle-in-a-box picture is particularly useful for the spinon, because it provides us with a framework with which we can numerically compute the spinon energy band.

The basic ideas are simple: by analogy with the solutions for a quantum particle in a box with free boundary conditions, we assume that we can sequentially label the excited modes of a single spinon in a finite-sized cluster with some quantum number n. Of course, for the same problem with periodic boundary conditions, this quantum number n is given by the wavevector k up to some constant, and we can always choose k to be our quantum number if we wish. Thus for each cluster size N, where N is equal to the number of triangles in the cluster, we obtain a set of single-spinon eigenvalues E_k^N and their corresponding quantum numbers k. We then make the fundamental assumption that the energy of a single spinon on the sawtooth lattice is a universal function of the parameter k/N, i.e. that it depends only on cluster size N and on the mode k of excitation for that cluster size. This assumption implies that we can numerically map out the spinon dispersion curve of (2.10*f*) if we plot out the energies E_k^N as a function of k/N. The dots in figure 6 represent such a plot; the curve which they delineate compares well with our analytical calculations. The latter were variational in nature, hence it is not surprising that they produce a curve which is higher in energy than that given by our numerical results. We have thus provided numerical proof of the existence of the spinon and antispinon excitations on the sawtooth lattice.

Let us complete the picture by reminding the reader of the numerical results which led to this paper. We found, via calculations on small clusters of topology I with periodic boundary conditions, that there was an energy gap between the ground state and the lowest band of excited states, and that in addition this lowest band had

total spin 1 and was flat. We hope we have been able to convince the reader that the states in this band can be understood in terms of one spinon and one antispinon excitation. It only remains for us to present numerical results which show that the flat energy spectrum is due to the two domain walls being independent of each other, with the antispinon localized somewhere on the lattice and the spinon delocalized away from the antispinon.

As mentioned briefly in the previous section, a flat energy band is rather unusual, and in this particular case we can only think of two possible causes of such a flat band, namely a localized spinon–antispinon excitation (cf (2.3)–(2.7)), *or* independent spinon and antispinon excitations in which the latter is localized and the former delocalized (cf (2.10)).

We can distinguish between the above two possibilities by numerically constructing a Wannier orbital out of eigenstates in the lowest band of excitations precisely in the manner described by (2.4) and (2.6), and then by examining spin–spin correlations in the Wannier orbital thus constructed. These calculations show explicitly that we do not have a localized spinon–antispinon wavepacket, but that at least one of the domain walls is delocalized. We are therefore forced to conclude that the domain walls must be independent of each other, in which case the only possible scenario for a flat energy spectrum is that in which the antispinon is localized somewhere on the lattice and the spinon is simultaneously delocalized away from the antispinon.

We conclude this section by thinking about excited states which contain more than one pair of spinon and antispinon domain walls. Using ideas discussed earlier in this subsection, it is clear that we can construct such a many-particle excitation by joining together 'chunks' of the sawtooth lattice with topologies of type I and II. However, in order for periodicity to prevail on the lattice, it is equally clear that we must connect topologies I and II alternately: it is not possible for two consecutive chunks of topology II to be joined up. Thus we are led to a picture of a higher excited state in which spinon excitations alternate with antispinon excitations (figure 11(*a*)). This is also the conclusion we reach if we apply the simple pictures for the spinon and antispinon domain walls which we used in our analytical work (figure 11(*b*)). Moreover, the spinons and antispinons in such a many-particle state cannot move past each other—they can only concertina against one another in accordance with our discussion at the end of section 2.1.

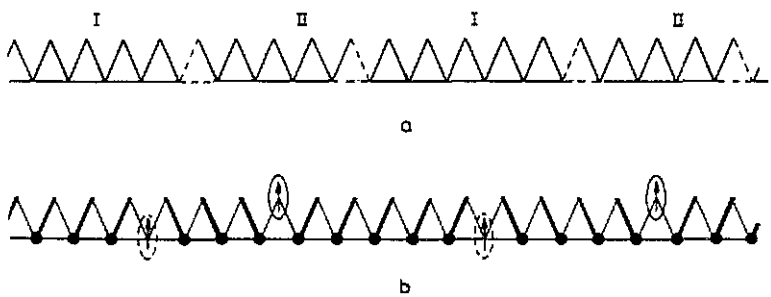

Figure 11. Pictorial representations of states containing multiple excitations. It is clear from topological considerations, as shown in figure 11(*a*), that clusters of topology type I must be alternately connected to clusters of topology type II. A clearer depiction of such a state is given in figure 11(*b*) with alternating spinon and antispinon excitations.

3. Class of models with a generic solution: holons alternating with spinons

We begin this section with the following conjecture: that our solutions for the Heisenberg model on the sawtooth lattice, consisting of a broken symmetry ground state of uncorrelated singlet pairs together with excited states that contain spin-$\frac{1}{2}$ spinons in alternating sequence with their conjugate excitations, the antispinons, are not restricted to this system alone but are in fact generic to an entire class of quasi-one-dimensional models. These models include some which contain mobile spinless charge carriers in addition to non-itinerant chargeless spins. In this section we discuss two such models, of interest in high-temperature superconductivity, for which the above conjecture is true.

The first is the t–J model on the sawtooth lattice (subsection 3.1), which contains not only the electronic spins that interact via Heisenberg exchange as already discussed, but also vacancies that can hop between the lattice sites. The ground state of the model in the presence of one vacancy is unchanged from that without any vacancies: we find uncorrelated, short-ranged singlet pairs which exhibit local broken symmetry. We also show that the excited states contain spin-$\frac{1}{2}$, chargeless spinons which alternate with their conjugate excitations; in this case the spinless, charge $+e$ holons.

We then introduce in subsection 3.2 the so-called X-model for the copper–oxygen (Cu–O) plane of perovskite superconductors, in which oxygen holes hop onto neighbouring oxygen sites via Cu^+ excitations. We discuss this model on a restricted geometry, namely the quasi-one-dimensional chain of copper–oxygen atoms that is found within each copper–oxygen plane (figure 12(a)). We solve for the X-model on this Cu–O chain by analogy with the t–J model on the sawtooth lattice, and argue that the ground states of both models consist of uncorrelated, short-ranged singlet pairs which exhibit the same broken symmetry. Further, we argue that our simple picture for the excited states of the t–J model, in which spinons alternate with their conjugates, is also valid for the Cu–O chain: excitations of the chain consist of spin-$\frac{1}{2}$, chargeless spinons alternating with spinless, charge $+e$ holons.

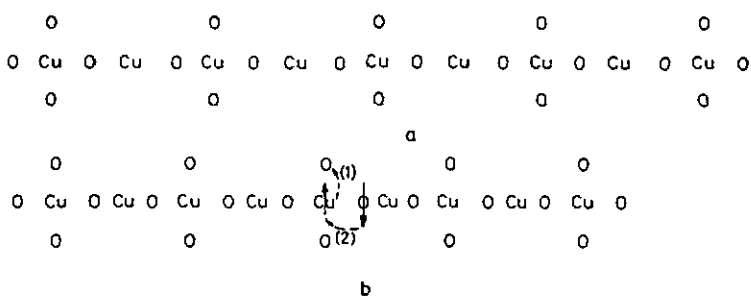

Figure 12. (a) The Cu–O chain discussed in section 3.2. (b) The oxygen hole hopping processes allowed in our X-model are depicted in this diagram. Each hopping process contains two stages: (i) the Cu hole hops onto an empty O site, generating Cu^+ excitations and (ii) its place is taken by an incoming O hole.

3.1. The t–J model on the sawtooth lattice

The t–J model is capable of describing the physical properties of magnetic insulators that contain mobile charged vacancies, and has therefore come under intense scrutiny

recently because of its possible relevance to the perovskites. The t–J Hamiltonian on an arbitrary lattice is given by

$$H = -t \sum_{\langle ij \rangle \sigma} \left(1 - c^{\dagger}_{i\sigma'} c_{i\sigma'}\right) c^{\dagger}_{i\sigma} c_{j\sigma} \left(1 - c^{\dagger}_{j\sigma'} c_{j\sigma'}\right) + J \sum_{\langle ij \rangle} \boldsymbol{S}_i \cdot \boldsymbol{S}_j \tag{3.1}$$

where $c^{\dagger}_{i\sigma'}$ as usual creates one electron at lattice site i with spin σ', $c_{i\sigma'}$ is its conjugate operator, the spins σ and σ' are conjugate to each other, $\boldsymbol{S}_i$ denotes the spin operator at the ith lattice site, and both summations are over all nearest-neighbour lattice sites. The first term describes the hopping of charged $+e$ vacancies between neighbouring lattice sites, the hopping energy being denoted by the parameter t. The presence of the pair of projection operators $(1 - c^{\dagger}_{l\sigma'} c_{l\sigma'})$ ensures that none of the lattice sites is doubly occupied in the hopping process. The magnetic properties of the system are described by the second term in Hamiltonian (3.1), which represents none other than the Heisenberg interactions between electronic spins on neighbouring lattice sites, with J denoting the exchange energy, as in the previous section.

It is not our intention here to discuss the t–J model in any generality, but we wish to point out that there are three free parameters in Hamiltonian (3.1), namely: (i) the topology of the underlying lattice; (ii) the number of vacancies in the system, or more precisely, their concentration; and (iii) the magnitude the dimensionless ratio t/J which, in turn, is set by the energy scales for hopping and Heisenberg exchange, respectively.

In the following discussion, we restrict our attention to the sawtooth lattice, and for this particular topology, we concentrate on solutions of the t–J model in the presence of a single charged vacancy or hole. The t–J model on the sawtooth lattice has been partially discussed in a previous paper; our aim here is to extend the discussion of Long and Fehrenbacher [11] by proving via simple physical arguments that this t–J model exhibits the generic solutions which form the main thrust of this article.

It is simplest and most illuminating to examine the above t–J model firstly in two obvious, extreme limits for the value of the ratio t/J, and then to proceed to general values of t and J. These two limits are firstly $t/J \to \infty$, where $t > 0$ and $J = 0$, and secondly $t/J = 0$, where $t = 0$ and $J > 0$.

In the former limit, in which $t > 0$ and $J = 0$ (i.e. $t/J \to \infty$), the Heisenberg term in the t–J Hamiltonian (3.1) drops out. Because there is no longer any explicit spin interaction present in the problem, one might naively have thought that the kinetic energy of the charged vacancy would be independent of the background spin configuration. This is not the case, however: the *nature* of the magnetic background is in fact crucial to the problem, and solving for the ground state of the model is equivalent to determining the spin correlations which minimize the hopping kinetic energy of the vacancy.

The above problem appears to have been first tackled by Nagaoka [12], who proved that the background spins on any bipartite lattice must be ferromagnetically correlated in order for the kinetic energy of a single vacancy hopping between the lattice sites to be minimized. However, Nagaoka's result does not necessarily hold for topologically frustrated lattices, where for instance antiferromagnetic correlations might be energetically more favourable. Indeed, in the case of the sawtooth lattice, we can prove both analytically and numerically that the hopping kinetic energy of a single vacancy is minimized in the presence of a spin background in which all spins are

paired up locally into short-ranged singlets, with no correlations whatsoever between any two pairs of singlets (as depicted in figure 13). Such a state is exactly reminiscent of the Heisenberg ground state described in section 2 (see figure 2).

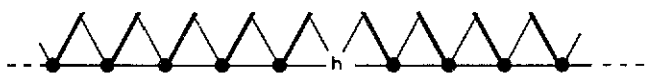

Figure 13. A component of the ground state of the t–J model on the sawtooth lattice. The lines in bold represent singlet correlations. The state shown is the exact ground state of the model for the hole h position indicated on the diagram.

There are three steps to understanding this result. Firstly, we observe that the smallest closed loop on the sawtooth lattice is a single triangle. Secondly, if we suppose that the single hole in our model is present in a particular triangle, then we note here that the hopping kinetic energy of the hole around that triangle is minimized if the two spins on the remaining lattice sites of the triangle are paired up into an exact singlet (see later). Finally, since the hole in our model can arrive at *any* triangle, it follows that the spins in all remaining triangles of the lattice should also be in exact, short-ranged singlet pairs, in order that the hopping kinetic energy of the hole be minimized everywhere on the lattice.

The above line of reasoning depends critically on our second assertion, which we now prove. Let us consider a single triangle containing one hole and two spins at its lattice sites,with none of the sites being doubly occupied. Suppose in the first instance that the two spins are parallel to one another and paired up as a triplet. There are three allowed states (see figure 14); one corresponding to each possible position of the hole. Using these states as a basis set, we can write the Hamiltonian (3.1) in matrix form as

$$H = \begin{bmatrix} 0 & t & t \\ t & 0 & t \\ t & t & 0 \end{bmatrix} \tag{3.2a}$$

which upon diagonalization, produces a ground state

$$|\Psi_0\rangle = (\tfrac{1}{2})^{1/2}[|i\rangle - |ii\rangle] \tag{3.2b}$$

(see figure 14 for notation) corresponding to a ground state energy

$$E_0 = -t. \tag{3.2c}$$

On the other hand, if we assume the two spins in the triangle to form a singlet bond, then there are still three possible states which form a basis set (see figure 15), but the t–J Hamiltonian now becomes

$$H = \begin{bmatrix} 0 & -t & -t \\ -t & 0 & -t \\ -t & -t & 0 \end{bmatrix} \tag{3.3a}$$

with the negative signs arising from the antisymmetry of the singlet pairs. The matrix (3.3a) leads, upon diagonalization, to a ground state (see figure 15) given by

$$|\Psi_g\rangle = (\tfrac{1}{3})^{1/2}[|1\rangle + |2\rangle + |3\rangle] \tag{3.3b}$$

which has as its corresponding eigenvalue

$$E_g = -2t. \tag{3.3c}$$

Consequently, the kinetic energy of a vacancy hopping around a triangle is halved if the spins on the remaining two lattice sites are forced into singlet pairing as opposed to triplet pairing. It can moreover be shown that there is a lower bound for the kinetic energy of a vacancy hopping on a lattice with coordination number z, and that this minimum kinetic energy is given by

$$E_{\min} = -zt. \tag{3.4}$$

Therefore, in the case of a single triangle, the lower bound on the kinetic energy of the hole is $-2t$, and the minimum is achieved by having singlet correlations between the spins in the triangle, thus proving our earlier assertion. The physical reason for singlet pairing being favourable for hole motion in a triangle is rather subtle [13]; we merely note here that in the t–J model, there is a phase factor of $-t$ associated with each hop of the hole *once* between any two nearest-neighbour sites, and that the presence of these phase factors means that hole motion around the triangle is in fact frustrated unless the spins in the triangle form a single.

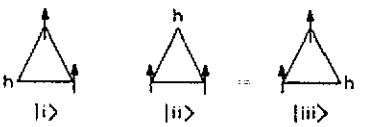

Figure 14. Set of basis states containing one hole and two parallel spins at the lattice sites of a single triangle.

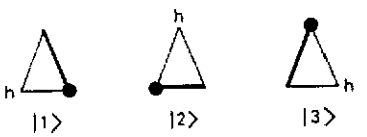

Figure 15. Set of basis states containing one hole and two antiparallel spins at the lattice sites of a triangle that are paired up into a singlet.

We have therefore shown the ground state of the t–J model on the sawtooth lattice, in the limit $t/J \to \infty$, to be a linear superposition of states such as that depicted in figure 13. However, such states are already familiar to us from section 2: it appears that for the sawtooth topology, the spin–spin correlations which are favourable for hole hopping are precisely those preferred by the Heisenberg exchange interaction between the spins themselves. Hence the full t–J model (i.e. when $t > 0$, $J > 0$) on the sawtooth lattice is exactly solvable: the ground state described in the preceding paragraph is unchanged when the Heisenberg exchange interaction J is 'switched on'.

Alternatively, we could begin by considering the Heisenberg model on the sawtooth lattice and asking about what happens when a single electronic spin is removed from the system, in the limit $t/J = 0$, i.e. when $t = 0$, $J > 0$. If one spin is removed, it is clear that at least one of the singlet pairs present in the ground state must break up. In fact, from our knowledge of the excitations of the Heisenberg model on the

sawtooth topology, we can immediately deduce that the hole acts as, or becomes, the antispinon excitation, since no energy is required for it to do so. In addition, we also know that there is a spin-$\frac{1}{2}$ spinon excitation present in the system, and that the hole and the spinon prefer to be well separated from one another. Because the same spin–spin correlations are favourable for both hole motion and Heisenberg interactions in the model, the picture we have just described is in fact little changed when the hole is given a finite, non-zero hopping kinetic energy (i.e. away from the limit $t/J = 0$): the hole and the spinon remain apart from each other, but the hole is free to delocalize around the spinon.

We have therefore proven that in the presence of a single vacancy, there are two elementary excitations in the t–J model on the sawtooth lattice which fall into distinct classes: a spinless, charge $+e$ hole excitation, or holon, and a spin-$\frac{1}{2}$, chargeless spin excitation, or spinon. The holon and spinon appear quite naturally to be well separated from one another in our model, thereby exhibiting the spin–charge separation one would expect. More generally, in the presence of many vacancies, we expect from our preceding discussion to find excited states which contain holons alternating with spinons. Hence the t–J model on the sawtooth lattice exhibits the same generic solutions as those discussed in the previous section.

3.2. The X-model for oxygen hole hopping on a copper–oxide chain

In this subsection, we discuss a model for oxygen hole hopping in the copper–oxygen planes of the perovskite superconductors; the so-called X-model mentioned earlier. In the X-model, each oxygen hole is allowed to hop onto any neighbouring oxygen site (and in principle back onto its initial site) via virtual Cu^+ excitations at the intermediate copper sites, in contrast to the t–J model where the transfer of oxygen holes is assumed to proceed via Cu^{3+} excitations. There is therefore an important conceptual difference between the two models: whilst the spin of an oxygen hole can effectively be ignored in the t–J model, in which case it is useful to regard the oxygen hole simply as a vacancy hopping in a spin background, the spin of each oxygen hole in the X-model plays a critical role in determining its physical properties and cannot be ignored. Consequently, an oxygen hole in the X-model must be thought of explicitly as carrying not only charge $+e$ but also spin $\frac{1}{2}$.

The Hamiltonian for the X-model is

$$H_X = X \sum_{\langle ij\rangle\sigma} \sum_{\langle ij'\rangle\sigma'} d^\dagger_{i\sigma} d_{i\sigma'} p^\dagger_{j'\sigma'} p_{j\sigma} \tag{3.5}$$

where $d^\dagger_{i\sigma}$ is an operator which creates one hole with spin σ at the ith copper sire, $p^\dagger_{j'\sigma'}$ creates one hole with spin σ' at the jth oxygen site, while $d_{i\sigma'}$ and $p_{j\sigma}$ are the respective Hermitian conjugates (with appropriate spins). In addition, the parameter X sets the hopping kinetic energy scale in the model. The oxygen hole hopping process, as described by the Hamiltonian of (3.5), therefore proceeds via intermediate copper sites, and contains two stages: the spin at the intermediate Cu site hops onto an allowed O site, thus generating a virtual Cu^+ excitation, but the latter is then immediately destroyed by the incoming O hole (figure 12(b)) whose spin replaces that of the missing spin on the Cu site.

Clearly, as mentioned previously, each oxygen hole can in principle hop *either* on to any of the oxygen sites neighbouring it *or* indeed onto its initial site. Our work

in this section assumes, however, that the latter possibility is excluded. This is an important constraint, which, together with a second crucial restriction (see below), enables us to obtain exact and simple solutions.

Our motivation for examining the X-model lies in the fact that x-ray photospectroscopy measurements [14] appear to indicate the importance of Cu^{+} excitations in the perovskites, and suggest that such excitations may well dominate over and above Cu^{3+} excitations. If that is the case, then it is clear that the X-model will provide a more realistic description of the high-temperature superconductors.

We discuss our constrained X-model—that is to say a model in which oxygen holes are allowed to hop *only* onto neighbouring oxygen sites—on a restricted sub-geometry of the copper–oxide plane. We choose as our sub-geometry the quasi-one-dimensional chain of the copper–oxygen atoms that is found within each of the planes (figure 12(a)). In particular, we solve for the X-model on one such Cu–O chain and show that its ground state in the presence of a single oxygen hole consists of uncorrelated, short-ranged singlet pairs of copper spins which exhibit the broken symmetry reminiscent of the sawtooth lattice solutions discussed previously. In addition, we demonstrate that our simple picture for the excited states of the Heisenberg model on the sawtooth topology, in which spinons alternate with their conjugates, is also valid for the X-model on the Cu–O chain: excitations in the latter consist of spin-$\frac{1}{2}$, chargeless spinons alternating with their conjugates, which in this case (as in the case of the t–J model discussed in the previous section) are spinless, charge $+e$ hole excitations or 'holons'.

Let us stress, however, that the above solutions are *not* general to the X-model on a chain of Cu and O atoms, but in fact require two constraints. Firstly, the geometry of the one-dimensional Cu–O chain must be precisely as shown in figure 12(a) [14]. Secondly, oxygen hole hopping within such a chain must be restricted so as to exclude the possibility of the oxygen holes hopping back onto their initial sites (cf earlier discussion).

It will be useful for our purposes to regard the Cu–O chain as being made up of units consisting of two elements: groups of four oxygen atoms surrounding one central copper atom, together with linear sequences of O–Cu–O atoms. We will refer to the former as clusters (figure 17(a)) and the latter as links (figure 18).

Solving for the X-model involves, as it did in the case of the t–J model, determining the nature of correlations between the Cu spins, induced as a result of oxygen hole hopping, which are in fact most favourable for the hopping of the oxygen hole. We can then prove by analogy with our arguments for the t–J model that the hopping kinetic energy of such an oxygen hole is minimized if spins at the Cu sites are paired up exactly into local singlets, with no correlations whatsoever between any two pairs of singlets (figure 16(a)). The state shown in figure 16(a) clearly has the same generic form as our previous solutions: to the left of the oxygen hole in figure 16(a), Cu spins at the centre of clusters are paired up with the Cu spins lying on links immediately to their right, while to the right of the oxygen hole, Cu spins at the centre of clusters form singlet pairs with the Cu spins lying on links immediately to the left of the clusters, thus exhibiting the broken symmetry reminiscent of the sawtooth lattice.

The arguments are as follows. In the X-model, a single O hole in the Cu–O chain of figure 12 is allowed to hop onto any of the O sites nearest it, so long as it does so via the intermediate Cu atoms, generating Cu^{+} excitations in the process. Hence in any one hop, such an oxygen hole can move within one of the two possible types of units which make up the chain, namely a cluster of atoms or a link (as previously

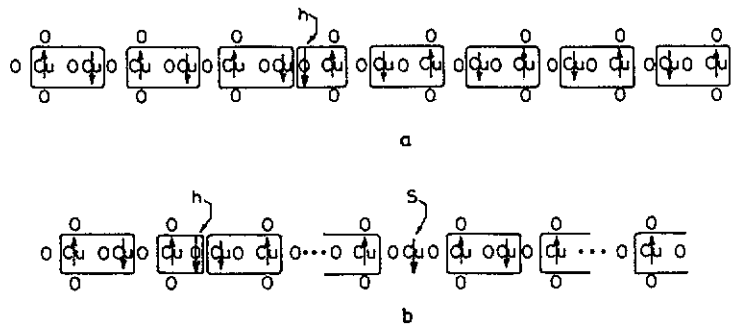

Figure 16. (*a*) A component of the ground state of our X-model on the Cu–O chain. The state shown is the exact ground state for the oxygen hole h position indicated. (*b*) A pictorial representation of an excited state of the Cu–O chain: excitations in our X-model consist of spinless, charge $+e$ holons (h) and spin-$\frac{1}{2}$, chargeless spinons (S).

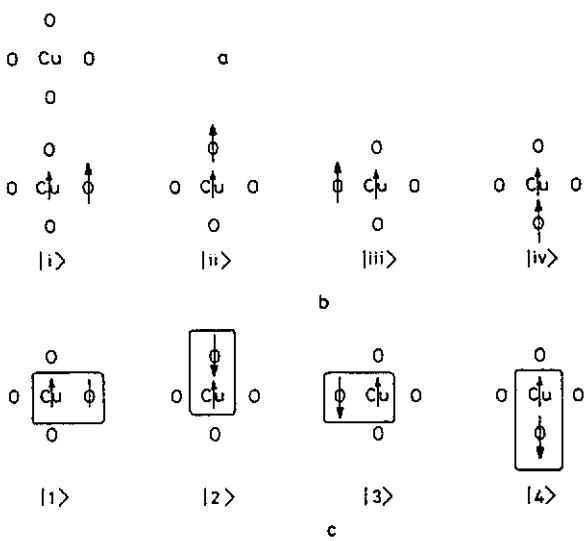

Figure 17. (*a*) A cluster of Cu–O atoms. (*b*) Set of basis states containing an O hole in parallel alignment with the Cu hole on a cluster of atoms. (*c*) Set of basis states containing an O hole in antiparallel alignment with the Cu hole such that they form a singlet pair.

O Cu O

Figure 18. A link of Cu–O atoms.

defined). For simplicity, let us in the first instance restrict ourselves to the case of oxygen hole hopping within a single cluster of atoms (figure 17(*a*)).

Within our constrained X-model, it is assumed that the single O hole is able to hop onto any of the three neighbouring O sites in the cluster. Suppose in the first instance that the spins of the O hole and the Cu electron are parallel to one another and form a triplet pair. Four such triplet states are possible (figure 17(*b*)), one corresponding to each allowed position of the oxygen hole. In that case, the

hopping of the O hole generates the following Hamiltonian for the X-model:

$$H_X = \begin{bmatrix} 0 & X & X & X \\ X & 0 & X & X \\ X & X & 0 & X \\ X & X & X & 0 \end{bmatrix}. \tag{3.6}$$

The matrix in (3.6) leads, upon diagonalization, to a ground state with energy $E_0 = -XX$. If, on the other hand we assume the spins of the oxygen hole and the copper electron to be antiparallel and to form a singlet pair, then there are once again obviously four such states which form a basis set (figure 17(*c*)), but we find that in this new basis, the Hamiltonian for the hopping of the oxygen hole in the X-model becomes

$$H_X = \begin{bmatrix} 0 & -X & -X & -X \\ -X & 0 & -X & -X \\ -X & -X & 0 & -X \\ -X & -X & -X & 0 \end{bmatrix}. \tag{3.7a}$$

The negative phases in the matrix elements above arise as a direct consequence of the antisymmetry of the singlet pairs and produce a ground state

$$|\Psi_g\rangle = (\tfrac{1}{4})^{1/2}[|1\rangle + |2\rangle + |3\rangle + |4\rangle] \tag{3.7b}$$

which has a corresponding eigenvalue of

$$E_g = -3X. \tag{3.7c}$$

Our results therefore show that the formation of a singlet pair between the spin of the O hole and that of the central Cu atom is more favourable for O hole hopping within the cluster than is the corresponding formation of a triplet pair. Moreover, it is clear from the general result expressed in (3.4) that the energy in (3.7*c*) above is in fact the minimum allowed kinetic energy for an oxygen hole hopping in such a cluster. We therefore conclude that the hopping kinetic energy of a single O hole within a cluster of atoms on the Cu–O chain is minimized via the formation of an exact O–Cu singlet.

Similarly, we can prove that the hopping of a single O hole within a link of O–Cu–O atoms (figure 18) is made most favourable by exact singlet pairing between the spins of the O hole and the Cu electron. In this instance, such pairing leads to a hopping kinetic energy for the O hole of $-X$, compared to the hopping energy of X which is returned by triplet pairing. We have therefore proven that exact singlet correlations are preferred locally by the O hole in our model.

We now observe that within the X-model, the oxygen hole can in principle hop into any cluster of the Cu–O chain, and that the total spin of atoms in each unit of cluster and link is conserved in this hopping process. Next, we note that the constraints in our model are such that the oxygen hole, no matter what its position along the Cu–O chain, is always able to minimize its kinetic energy by forming an *exact* singlet pair with a local copper spin. Such low-spin correlations, favoured locally by the oxygen hole, must be conserved in the process of oxygen hole hopping in accordance with our previous observation. It therefore follows that in hopping

through the Cu–O chain, the charge $+e$ oxygen hole in our model effectively leaves behind a trail of Cu spins which are paired up into exact, local singlet pairs, giving rise to the state depicted in figure 16(*a*). We emphasize once again that this result is not general to the X-model, but is obtained provided the two essentially topological constraints described earlier are imposed.

Moreover, the doped oxygen hole, which carries a spin of $\frac{1}{2}$ in addition to a charge of $+e$, must necessarily also leave behind one unpaired spin-$\frac{1}{2}$ Cu spin in the chain (see figure 16(*b*)). It can be seen from figure 16(*b*) that this must be the case on the grounds of periodicity, with the unpaired Cu spin being parallel with the spin of the O hole. Our preceding analysis indicates that it would in fact be energetically unfavourable for the unpaired Cu spin to be near the O hole, and we therefore expect them to be well separated. Furthermore, the existence of one unpaired Cu spin implies the breaking up of at least one of the many consecutive singlet pairs in the ground state, which must in turn incur a finite, non-zero energy cost. In the context of our previous discussion, we can identify the unpaired Cu spin as a spin-$\frac{1}{2}$, chargeless spin excitation, or spinon, and the O–Cu singlet in figure 16(*b*) as a spinless, charge $+e$ hole excitation, or holon.

We have therefore shown that in the presence of a single O hole, the lowest-lying solutions for the X-model on the Cu–O chain fall into the same generic class as those of the t–J model on the sawtooth lattice: there is a broken-symmetry ground state consisting of uncorrelated, short-ranged singlet pairs of Cu spins together with two classes of excitations, namely spin-$\frac{1}{2}$, chargeless spinons and spinless, charge $+e$ holons. It is clearly conceivable that other models may be found which exhibit the same generic solutions, as we conjectured at the beginning of this section.

However, because the two types of excitations in these models must alternate with one another as a result of topological constraints, this unfortunately means that the class of model under discussion in this article can never undergo a superconducting transition: holons in any excited state must alternate with spinons and two holons cannot therefore approach each other. On the other hand, should topological constraints be lifted, there appears to be no *a priori* reason to exclude the possibility of the holons in these models pairing up in some way. Work on constructing two-dimensional systems with simple ground states is therefore continuing.

4. Summary and conclusions

In this paper, we have discussed a topologically frustrated spin-$\frac{1}{2}$ quantum mechanical Heisenberg model with unusually simple solutions: its doubly degenerate broken-symmetry ground state is exactly dimerized, and there is an energy gap to its excitations. We interpret the excitation gap as being due to the formation of two (chargeless) spin-$\frac{1}{2}$ domain walls. Because of a topological asymmetry in our model, the domain walls fall into *two classes*: one class (spinons) incurs an energy penalty, whilst the second (antispinons) costs no energy to create. Moreover, we shown that there are high-T_c models which exhibit the same generic solutions as those found in our frustrated magnet. In particular, we concentrate on a d–p model containing a single oxygen vacancy which we solve on a sub-geometry of the copper–oxide plane of the perovskite superconductors. We show that the ground state of our d–p model contains uncorrelated, short-ranged copper singlet pairs, whilst excitations in the model consist of chargeless spin-$\frac{1}{2}$ domain walls or 'spinons', together with charge $+e$ spinless hole excitations or 'holons'.

References

[1] Mattis D C 1981 *The Theory of Magnetism I (Springer Series in Solid-State Sciences 17)* (Berlin: Springer)
Caspers W J 1989 *Spin Systems* (Singapore: World Scientific)
[2] Goldstons J 1961 *Nuovo Cimento* **19** 154
[3] Broholm C, Aeppli G, Espinosa G P and Cooper A S 1990 *Phys. Rev. Lett.* **65** 3173
[4] Anderson P W 1973 *Mater. Res. Bull.* **8** 153
[5] Anderson P W 1987 *Science* **235** 1196
[6] Yang B X, Mitsuda S, Shirane G, Yamaguchi Y, Yamauchi H and Syono Y 1987 *J. Phys. Soc. Japan* **56** 2283
Freltoft T, Fischer J E, Shirane G, Moncton D E, Sinha S K, Vaknin D, Remeika J P, Cooper A S and Marshman D 1987 *Phys. Rev.* B **36** 826
Yamada K, Kudo E, Endoh Y, Hidaka Y, Oda M, Suzuki M and Murakami T 1987 *Solid State Commun.* **64** 753
[7] Birgeneau R J *et al* 1988 *Phys. Rev.* B **38** 6614
Birgeneau R J, Endoh Y, Kakurai K, Hidaka Y, Murakami T, Kastner M A, Thurston T R, Shirane G and Yamada K 1989 *Phys. Rev.* B **39** 2868
[8] Shirane G, Birgeneau R J, Endoh Y, Gehring P, Kastner M A, Kitazawa K, Kojima H, Tanaka I, Thurston T R and Yamada K 1989 *Phys. Rev. Lett.* **63** 330
Rossat-Mignod J 1991 *Proc. Low Temp. Phys. Conf.; Physica* B **169**
[9] Warren W W *et al* 1989 *Phys. Rev. Lett.* **62** 1193, and references therein
[10] Haldane F D M 1983 *Phys. Lett.* **93A** 464
Affleck I, Kennedy T, Lieb E H and Tasaki H 1987 *Phys. Rev. Lett.* **59** 799
Majumdar C K and Ghosh D K 1969 *J. Math. Phys.* **10** 1388;1969 *J. Math. Phys.* **10** 1399
Shastry B S and Sutherland B 1981 *Phys. Rev. Lett.* **47** 964
[11] Long M W and Fehrenbacher F 1990 *J. Phys.: Condens. Matter* **2** 2787
[12] Nagaoka Y 1966 *Phys. Rev.* **147** 392
[13] Fehrenbacher F 1990 *Diplomarbeit* Bodensee Universität Konstanz
[14] For example, our solutions cease to hold in the case of a Cu–O chain in which *all* copper atoms are surrounded by four oxygen atoms